Full paper

New Phytologist

WOX9 functions antagonistic to STF and LAM1 to regulate leaf blade expansion in *Medicago truncatula* and *Nicotiana sylvestris*

Tezera W. Wolabu[1,2], Hui Wang[1,3], Dimiru Tadesse[1], Fei Zhang[1,4], Marjan Behzadirad[1], Varvara E. Tvorogova[1,5], Haggag Abdelmageed[1,6], Ye Liu[7], Naichong Chen[1,8], Jianghua Chen[9], Randy D. Allen[1,8] and Million Tadege[1,10]

[1]Institute for Agricultural Biosciences, Oklahoma State University, Ardmore, OK 73401, USA; [2]Noble Research Institute, LLC, Ardmore, OK 73401, USA; [3]College of Grassland Science and Technology, China Agricultural University, Beijing 100193, China; [4]Department of Molecular, Cellular and Developmental Biology, Yale University, New Haven, CT 06520-8104, USA; [5]Department of Genetics and Biotechnology, St Petersburg State University, St Petersburg 199034, Russia; [6]Department of Agricultural Botany, Faculty of Agriculture, Cairo University, Giza, 12613, Egypt; [7]School of Life Science, University of Science and Technology of China, Hefei, Anhui 230027, China; [8]Department of Biochemistry and Molecular Biology, Oklahoma State University, Stillwater, OK 74078, USA; [9]CAS Key Laboratory of Tropical Plant Resources and Sustainable Use, CAS Center for Excellence in Molecular Plant Sciences, Xishuangbanna Tropical Botanical Garden, Chinese Academy of Sciences, Kunming, Yunnan 650223, China; [10]Department of Plant and Soil Sciences, Oklahoma State University, Stillwater, OK 74078, USA

Author for correspondence:
Million Tadege
Email: million.tadege@okstate.edu

Received: *10 August 2020*
Accepted: *7 September 2020*

New Phytologist (2021) **229:** 1582–1597
doi: 10.1111/nph.16934

Key words: cell proliferation, leaf blade development, leaf polarity, *Medicago truncatula*, *Nicotiana sylvestris*, STF, WOX genes, WOX9.

Summary

- WOX family transcription factors regulate multiple developmental programs. The intermediate clade transcriptional activator WOX9 functions together with the modern clade transcriptional repressor WOX genes in embryogenesis and meristems maintenance, but the mechanism of this interaction is unclear.
- *STF* and *LAM1* are WOX1 orthologs required for leaf blade outgrowth in *Medicago truncatula* and *Nicotiana sylvestris*, respectively. Using biochemical methods and genome editing technology, here we show that *WOX9* is an abaxial factor and functions antagonistically to *STF* and *LAM1* to regulate leaf blade development.
- While *NsWOX9* ectopic expression enhances the *lam1* mutant phenotype, and antisense expression partially rescues the *lam1* mutant, both overexpression and knockout of *NsWOX9* in *N. sylvestris* resulted in a range of severe leaf blade distortions, indicating important role in blade development. Our results indicate that direct repression of *WOX9* by WUS clade repressor STF/LAM1 is required for correct blade architecture and patterning in *M. truncatula* and *N. sylvestris*.
- These findings suggest that controlling transcriptional activation and repression mechanisms by direct interaction of activator and repressor WOX genes may be required for cell proliferation and differentiation homeostasis, and could be an evolutionarily conserved mechanism for the development of complex and diverse morphology in flowering plants.

Introduction

WUSCHEL-related homeobox (WOX) factors are plant-specific transcriptional regulator proteins that contain a DNA binding homeodomain similar to WUSCHEL (WUS), the founding member of the family from Arabidopsis. Several elegant studies demonstrated that the WOX family is involved in the regulation of a wide range of key developmental programs. While WOX2, WOX8, and WOX9 function in zygotic development and embryogenesis (Haecker *et al.*, 2004; Breuninger *et al.*, 2008; Ueda *et al.*, 2011), WUS and WOX5 modulate stem cell maintenance in shoot and root apical meristems, respectively (Mayer *et al.*, 1998; Sarkar *et al.*, 2007). WOX1 and/or WOX3/PRS, however, orchestrate leaf blade and floral organ development as demonstrated in several species (Matsumoto & Okada, 2001; Nardmann *et al.*, 2004; Park *et al.*, 2005; Shimizu *et al.*, 2009; Vandenbussche *et al.*, 2009; Tadege *et al.*, 2011a; Nakata *et al.*, 2012; Zhuang *et al.*, 2012; Cho *et al.*, 2013; Ishiwata *et al.*, 2013; Niu, 2018).

WUS and its homologs in other species, including *TERMINATOR* (*TER*) in petunia, *ROSULATA* (*ROA*) in Antirrhinum, and *HEADLESS* (*HDL*) in Medicago, are required for shoot apical meristem (SAM) maintenance (Laux *et al.*, 1996; Mayer *et al.*, 1998; Stuurman *et al.*, 2002; Kieffer *et al.*, 2006; Meng *et al.*, 2019; Wang *et al.*, 2019). Loss of *WUS* function in the *wus-1* Arabidopsis mutant results in premature termination and arrest of the SAM and floral meristem (FM), but the SAM re-establishes itself to resume growth while the process repeats

itself, leading to altered plant morphology (Laux *et al.*, 1996; Mayer *et al.*, 1998). In the *hdl* mutant of *Medicago truncatula*, the terminated SAM is never fully re-established, and the few meristematic cells that try to re-establish are consumed in making leaves. As a result, *hdl* plants make only leaves throughout development (Tadege *et al.*, 2015; Meng *et al.*, 2019; Wang *et al.*, 2019). The *hdl* mutant also shows altered leaf shape (Meng *et al.*, 2019; Wang *et al.*, 2019), which was not detected in the *wus* mutant. However, the *wus wox1 prs* triple mutant showed a stronger leaf phenotype than the *wox1 prs* double mutant (Zhang & Tadege, 2015), suggesting that WUS may also have a redundant function in leaf development. Although *WUS* transcript is specifically expressed in the organizing center (OC) of the SAM (Mayer *et al.*, 1998), it is likely that a noncell autonomous signal from WUS may contribute to blade outgrowth, since the WUS protein itself is shown to move from the OC to the stem cell region (Yadav *et al.*, 2011; Daum *et al.*, 2014).

An intimate connection exists between WUS and the phytohormone cytokinin, and this appears to be true for STF/WOX1 as well (Tadege & Mysore, 2011; Tadege, 2016; H. Wang *et al.*, 2017). While WUS activity is modulated by cytokinin in the SAM and axillary meristem (J. Wang *et al.*, 2017; Snipes *et al.*, 2018), WUS promotes cytokinin activity in the shoot stem cell niche by repressing type-A *ARABIDOPSIS RESPONSE REGULATOR* (*ARR*) genes *ARR5*, *ARR6*, *ARR7*, and *ARR15* (Leibfried *et al.*, 2005) to activate cell proliferation. The WUS SAM maintenance activity and interaction with cytokinin were shown to be linked to its WUS box (Ikeda *et al.*, 2009; Dolzblasz *et al.*, 2016; Snipes *et al.*, 2018), suggesting that WUS primarily functions as a transcriptional repressor. Interestingly, *WUS* is reported to be activated by WOX9/STIP, which is also required for shoot meristem maintenance (Wu *et al.*, 2005) and embryo development (Wu *et al.*, 2007; Ueda *et al.*, 2011). However, WOX9 is reported to be a strong transcriptional activator (Lin *et al.*, 2013a), and it is unclear whether WUS and WOX9 employ the same mechanism in shoot meristem maintenance.

The *WOX9* gain-of-function *stip*-D mutant displays wavy leaf margins (Wu *et al.*, 2005), and the *stip* loss-of-function mutant is arrested at the seedling stage (Wu *et al.*, 2005), but it is unclear if *WOX9/STIP* plays a significant role in leaf blade development. The *WOX* genes that function in leaf blade development belong to the WUS clade transcriptional repressors as exemplified by *WOX1* and *PRS/WOX3* in Arabidopsis (Vandenbussche *et al.*, 2009; Nakata *et al.*, 2012), *STF* in *M. truncatula*, and *LAM1* in *Nicotiana sylvestris* (Tadege *et al.*, 2011a). Unlike leaf polarity factors that are either adaxial or abaxial-specific (Waites *et al.*, 1998; Sawa *et al.*, 1999; Siegfried *et al.*, 1999; Kerstetter *et al.*, 2001; McConnell *et al.*, 2001; Iwakawa *et al.*, 2002), the WOX genes *STF*, *WOX1,* and *PRS* are expressed in the middle at the adaxial–abaxial juxtaposition to control mediolateral outgrowth of the leaf blade (Tadege *et al.*, 2011a; Tadege *et al.*, 2011b; Nakata *et al.*, 2012; Nakata & Okada, 2012), suggesting a novel mechanism for blade expansion.

STF/LAM1 is a transcriptional repressor (Lin *et al.*, 2013a,b) and its repression activity is conferred by its WUS box and STF box motifs (Zhang *et al.*, 2014; Zhang & Tadege, 2015). The DNA binding STF homeodomain (HD) and the repression motifs (WUS box and STF box) are critically required for blade outgrowth function (Lin *et al.*, 2013a; Zhang *et al.*, 2014, 2019). Interestingly, all of the WUS clade Arabidopsis WOX transcription factors (WUS and WOX1–WOX7), which have transcriptional repression activity, can substitute for *LAM1* function (Lin *et al.*, 2013a), suggesting that modern/WUS clade WOX members have a conserved transcriptional repression mechanism in meristem maintenance and lateral organ development, with specificity conferred by cis elements that drive specific expression patterns.

Intermediate clade WOX members have intact HD but lack repression domains. Here we show that homologs of the intermediate clade transcriptional activator WOX9, namely, MtWOX9-1, MtWOX9-2 and NsWOX9, function antagonistically to STF or LAM1, and exacerbate the *lam1* phenotype when overexpressed. Suppression of *NsWOX9* transcript levels by antisense technology partially rescues the *lam1* mutant leaf blade phenotype while the introduction of knockout mutations in the native *NsWOX9* gene by multiplex gRNA genome editing severely affected leaf blade symmetry and expansion. Our results suggest that direct and antagonistic interactions between transcriptional repressor and activator *WOX* genes may be important to maintain homeostasis in cell proliferation and differentiation in acquiring complex morphology in flowering plants.

Materials and Methods

Plant materials and growth conditions

Plant materials used for this study including *M. truncatula* R108, *stf* mutant (*stf-2*), and *N. sylvestris* wild type (WT) and *lam1* mutant were grown in one gallon pots in a glasshouse under long-day (LD) conditions with 16 h : 8 h, light : dark cycle at 23–27°C, and in growth room under LD conditions of 16 h : 8 h, light : dark cycle at 23–25°C, 70–80% relative humidity, and a light intensity of 150 μmol m^2.

Samples collection, RNA extraction

Medicago truncatula tissue samples were collected from 4-wk-old WT and *stf* mutant plants. For GR induction, 4-wk-old plants of *p35S::YFP-GR-STF, p35S::YFP-GR-LAM1* and *p35S::YFP-GR-NsWOX9* transgenic lines were treated with mock, DEX (10 mM), and CHX (10 mM) for 3 h in *M. truncatula* and 6 h in *N. sylvestris*, before leaf samples were collected. Collected samples were immediately snap-frozen in liquid nitrogen and stored at −80°C until processing. Total RNA from shoot apex and young leaf of *M. truncatula* R108 (WT) and *stf-2* mutant, *N. sylvestris* (WT) and *lam1* mutant, Arabidopsis L*er* (WT), *wox1 prs* double mutant and *p35S::YFP-GR-STF, p35S::YFP-GR-LAM1* and *p35S::YFP-GR-NsWOX9* transgenic lines were isolated using TRIzol Reagent (Invitrogen, Carlsbad, CA, USA) for cDNA synthesis.

Real-time PCR

Expression patterns analyses were performed using quantitative real time polymerase chain reaction (qPCR) and semi-quantitative PCR with specific forward and reverse primers (Supporting Information Table S1). Reverse transcription (RT) was performed using RNA treated with DNase I (Invitrogen), an oligo (dT) primer, and SuperScript III reverse transcriptase (Invitrogen) according to the manufacturer's instruction. The RT-qPCR assays were performed with three biological and three technical replicates using SYBR Green real-time PCR Master Mix (Invitrogen). *Medicago truncatula*, Arabidopsis and *N. sylvestris* actin primers were used as standards. All specific forward and reverse primers used for gene cloning and expression and related molecular analyses in this study are listed in Table S1.

Gene isolation and transgene construction

MtWOX9-1 and *MtWOX9-2* genes were isolated from the *M. truncatula* genome by BLAST search using the AtWOX9 sequence. Full-length *MtWOX9-1* and *MtWOX9-2* coding sequences were amplified by RT-PCR using total RNA extracted from leaf samples, and constructs were made via gateway cloning using pDONR207 and pMDC32 vectors. The resulting plasmids were transferred into *Agrobacterium tumefaciens* strains *AGL1* and *GV2260* for *M. truncatula* and *N. sylvestris*, respectively, transformation as previously described (Tadege *et al.*, 2011a). For *WOX9* antisense (*NsWOX9-anti*) construct, *NsWOX9-anti-F* and *NsWOX9-anti-R* primers were used to amplify the full length CDS from the *NsWOX9-cDNA* and clone into the Gateway vectors. All generated transgenic lines were confirmed by PCR using specific primers, and reduced expression lines were identified by RT-PCR.

Multiplex gRNA-CRISPR/Cas9 construction

To generate the multiplex gRNA-CRISPR/Cas9 *NsWOX9* construct, we designed three multiplex gRNAs targeting multiple sites of exon 2 (gRNA1-CTTCAAGAATATGGCCA AGT; gRNA2-CTTCAAGAATATGGCCAAGT and gRNA3-TCTCCTGCTGTTATCA CACA) at the upstream of PAM (TGG, TGG, and AGG) sites, respectively, using the web-based tool CRISPR-P (http://cbi.hzau.edu.cn/cgi-bin/CRISPR; Lei *et al.*, 2014). All designed gRNAs were inserted between tRNA and gRNA scaffolds and clustered in tandem using the Golden Gate assembly method (Engler *et al.*, 2008). The pGTR plasmid, which contains a tRNA-gRNA fragment, was used as a template to synthesize polycistronic tRNA-gRNA (PTG) (Xie *et al.*, 2015). The overlapping PCR products were separated and purified by the Spin Column PCR Product Purification Kit (Wizard SV Gel and PCR Clean-Up System) following manufacturer's instruction (Promega, Madison, WI, USA). Then, the chain of multiplex tRNA-gRNA with three *NsWOX9*-spacers was inserted into an optimized vector with AtU6-tRNA-gRNAs-AtUBQ10-Cas9-pRGEB31-bar backbone by digestion and ligation using *Fok I* (NEB) and *BsaI* enzymes (Xie *et al.*, 2015). Target gRNAs and primers used in this study are listed in Table S1.

CRISPR/Cas plant transformation and analysis

The subsequent multiplex *NsWOX9spacer*-gRNA-CRISPR/Cas9 binary vector construct was transformed into *Agrobacterium* strain *GV2260*. First, transgenic lines were screened by PCR using genomic DNA and specific primers (PPT-F+PPT-R) of Barsta selection marker. Then, putative *Nswox9-CRISPR* mutants were identified through amplification of the target region by PCR using extracted genomic DNA as a template with specific primers designed from the border of the target site. Amplified fragments of the mutated region were sub-cloned into pGEM-T easy plasmid by TA-Cloning and 10 colonies for each locus were subjected to Sanger sequencing. Reads were analyzed by aligning with the reference sequence using the SeqMan Pro 15.0.1 (DNASTAR software for life scientists) (https://www.dnastar.com/quote-request/).

Electrophoretic mobility shift assay

The *MtWOX9-1* promoter with 37, 30 and 32 bp oligonucleotides, corresponding to starting sites at −22, −226 and −491, respectively, upstream of the start codon were labeled using the Biotin 3′ End DNA Labeling Kit according to the manufacturer's instructions (Thermo Scientific/Pierce, Waltham, MA, USA). Electrophoretic mobility shift assay (EMSA) was performed using Light Shift Chemiluminescent EMSA Kit (Thermo Scientific/Pierce). Unlabeled probes with a 50-fold higher concentration were used as competitors in each of the competing assays. Purified maltose binding protein (MBP) and MBP-STF were used in the EMSA on 10% native polyacrylamide gels as described (Zhang *et al.*, 2014). The biotin-labeled DNA was detected by chemiluminescence and exposed to X-ray film (Kodak, Rochester, NY, USA).

Chromatin immunoprecipitation (ChIP) assays

Chromatin immunoprecipitation (ChIP) assays were performed as described previously (Xiong *et al.*, 2013; Chen *et al.*, 2018). Protoplast extracted from 14-d-old *pMtWOX9-1:MtWOX9-1/wox1prs* transgenic Arabidopsis leaves were transformed with 10 µg of *35S::STF-YFP* using the polyethylene glycol-mediated transformation method. Protoplast crosslinking, chromatin isolation and preclearing were performed as described (Chen *et al.*, 2018). Precleared chromatins were incubated with 5 µl of anti-GFP antibody (ab290) overnight at 4°C, after which Protein A agarose beads (40 µl) were added, and the samples were incubated at 4°C for 2 h. After reversing the crosslinks with Proteinase K at 65°C overnight, DNA was purified and analyzed by qPCR amplification using specific primers. The input DNA and HA antibody-precipitated DNA were used as PCR templates for the positive and negative controls, respectively. Experiments were repeated three times.

Dual luciferase assay

For effector plasmids, the coding sequence of *STF* or GUS was cloned into pDONR207 entry vector and then transferred into p2GW7 using the Gateway system (Invitrogen). Construction of the reporter *pMtWOX9-1-mini-35S-LUC* plasmid containing 1 kb of the *MtWOX9-1* promoter was performed as previously described (Zhang *et al.*, 2014). Transient expression assays were performed in Arabidopsis protoplasts as described (Asai *et al.*, 2002). For normalization, 0.5 μg of plasmid pRLC was used as an internal control.

Histological analysis

Leaf samples were fixed in formaldehyde for 48 h and dehydrated in an ethanol series (60%, 70%, 85% and 95%). Then, leaves were embedded in Paraplast (Sigma-Aldrich, St Louis, MO, USA) and tissue sections (15 μm thick) were cut with a Reichert-Jung 2050 microtome. Specimens were mounted on slides and stained with Safranine O and Light Green as previously described (Tadege *et al.*, 2011a). Images were captured with digital camera mounted on an Olympus BX-51 compound microscope.

RNA *in situ* hybridization

Templates of RNA probes were derived from *MtWOX9-1* cDNA with gene specific primers containing T7 promoter sequence at the 5′ end, and the RNA probes were end-labeled with DIG oligonucleotide 3′ end-labeling kit. The vegetative shoot buds of 3-wk-old R108 plants grown in a glasshouse under LD conditions were used for RNA *in situ* hybridization. *In situ* hybridization was performed according to a standard protocol (Weigel & Glazebrook, 2002).

Sequence alignment and phylogenetic tree construction

Multiple protein sequence alignment was performed using BioEdit software and the ClustalW program. Species refer to At (*Arabidopsis thaliana*), Ns (*Nicotiana sylvestris*), Pc (*Phaseolus coccineus*), Gm (*Glycine max*), Vv (*Vitis vinifera*), Ph (*Petunia* × *hybrid*), Cs (*Cucumis sativus*), Sl (*Solanum lycopersicum*) and Ca (*Capsicaum annuum*). A neighbor-joining phylogenic tree was constructed using MEGA-X default settings with 1000 bootstrap replications.

Accession numbers

Sequence data from this article can be found in the National Center for Biotechnology Information (NCBI) Genbank database, or *M. truncatula* Genome Database (http://www.medicagogenome.org/).

Corresponding to: MtWOX9-1, Medtr2g015000; MtWOX9-2, Medtr7g026130; AtWOX9, AT2G33880; AtWOX8, AT5G45980; NsWOX9, XM_009794999; NsLAM1, AEL30893; MtSTF, JF276252; AtWOX1, AT3G18010; AtWOX3/PRS, AT2G28610; PcWOX9, ACL11801; GmWOX9, XP_006594207; GmWOX9, XP_003541514; VvWOX9, XP_002273188; Ca WOX9, XP_016562050; CsWOX9, XP_004134676; PhEVG, ABO93066; PhSOE; ABO93067; SlWOX9/S, NP_001234072.

Results

Ectopic expression of *WOX9* enhances the *stf* and *lam1* mutant phenotypes

We have previously shown that, while the WUS clade repressor *WOX* genes of Arabidopsis including *WUS* and *WOX1*–*WOX7* complement the *lam1* mutant phenotype when driven by the *STF* promoter, the intermediate clade *WOX9* expression exacerbates the *lam1* mutant phenotype (Lin *et al.*, 2013a). Therefore, we decided to investigate whether the unique activity of *WOX9* is conserved in *M. truncatula* and *N. sylvestris* and determine its biological significance in leaf development. We isolated orthologous coding sequences for *AtWOX9* from *M. truncatula* (*MtWOX9*) and *N. sylvestris* (*NsWOX9*) and created expression constructs that placed these sequences under control of the *STF* promoter to ectopically express these genes in the *stf-2* and *lam1* mutant plants. The *STF* promoter drives expression specifically at the adaxial–abaxial juxtaposition of leaf primordia in *M. truncatula* (Tadege *et al.*, 2011a) similar to the expression pattern of *WOX1* in Arabidopsis (Nakata *et al.*, 2012). *Stf-2* and *lam1* are severe leaf blade mutants in *M. truncatula* and *N. sylvestris*, respectively, caused by mutation of the *WOX1* orthologs *STF* and *LAM1* (Fig. 1b,e). The *M. truncatula* genome contains two *WOX9*-like sequences here designated as *MtWOX9-1* and *MtWOX9-2* (Supporting Information Figs S1, S2). We introduced *MtWOX9-1* driven by the *STF* promoter (*STF::MtWOX9-1*) first into the *stf-2 M. truncatula* plants and eight independent transgenic lines were generated. Expression of *MtWOX9-1* in the *stf-2* mutant background was confirmed by RT-PCR assays. All of these transgenic lines displayed strongly enhanced mutant phenotype with much narrower leaves and thinner stems compared to the *stf* mutant (Fig. 1a–c). In addition, leaves and stems were significantly shorter in length, leading to a dwarf phenotype that was not characteristic of the *stf* mutant phenotype (Fig. 1b,c). Similarly, introduction of this construct into the *lam1* mutant background severely affected both leaf length and width, exacerbating the *lam1* mutant phenotype (Fig. 1d–f). These results indicate that both the *stf* and *lam1* mutants respond similarly to the activity of *MtWOX9-1,* consistent with the effect of *AtWOX9* expression driven by the *STF* promoter in the *lam1* mutant (Lin *et al.*, 2013a). We also transformed *35S::MtWOX9-1, 35S::MtWOX9-2* and *35S::NsWOX9* into the *lam1* mutant and obtained severely enhanced mutant phenotypes similar to the *STF::MtWOX9-1* expressing *lam1* lines (Fig. 1g–i), indicating that these three genes have similar effects on leaf blade outgrowth. In most cases, these transgenic leaves displayed approximately five-fold reduction in leaf length, but this effect appeared to be dependent on the level of *WOX9* transgene expression since plants with high level of transgene expression showed more severe phenotypes compared to *lam1* plants with low level of transgene expression (Fig. S3).

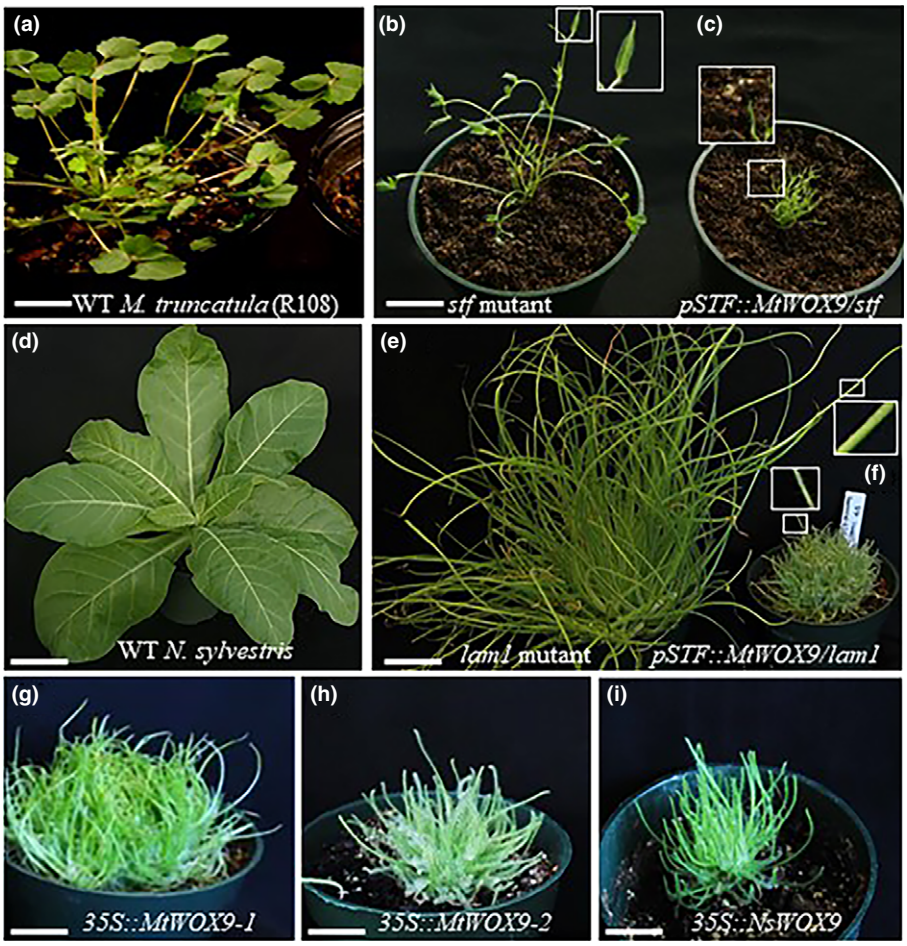

Fig. 1 Ectopic expression of *WOX9* enhances *stf* and *lam1* mutant phenotypes. (a) Untransformed *Medicago truncatula* wild type (WT) (R108) plant. (b) Phenotype of untransformed *stf* mutant. (c) *stf* mutant transformed with *STF::MtWOX9-1*. (d) Untransformed *Nicotiana sylvestris* WT plant. (e) Phenotype of untransformed *lam1* mutant. (f) *lam1* mutant transformed with *STF::MtWOX9-1*. Insets in (b), (c), (e) and (f) show magnified areas of individual leaves. (g) *lam1* mutant transformed with *35S::MtWOX9-1*. (h) *lam1* mutant transformed with *35S::MtWOX9-2*. (i) *lam1* mutant transformed with *35S::NsWOX9*. Plants were 10-wk (e and f) or 5-wk old (all the rest). Bars, 10 cm.

The enhancement of *stf* and *lam1* mutant phenotypes associated with WOX9 expression suggested to us that *WOX9* acts in opposition to *STF/LAM1* in leaf blade development. Therefore, we introduced an *NsWOX9-antisense* construct into the *lam1* plants to see if reduced levels of *NsWOX9* transcripts could alleviate the mutant phenotype. Indeed, expression of an *NsWOX9-antisense* construct had the opposite effect of *NsWOX9* overexpression, partially rescuing the *lam1* mutant leaf phenotype (Fig. 2). However, this partial complementation was limited, and the antisense plants still appeared bushy and failed to make stems. Nonetheless, unlike the untransformed *lam1* mutant control, the *NsWOX9-antisense* leaves showed distinct petioles and blades especially at early stages of development (Fig. 2a,b), and the blades were variously branched and curled resulting in unusual leaf structure at maturity (Fig. 2c–e). These leaf phenotypes suggest that blade outgrowth initiation has significantly progressed in the *NsWOX9-antisense* plants but perhaps aborted before completion.

To more completely evaluate the effects altered WOX9 expression on the *lam1* mutant phenotype, we carried out structural examination of leaf tissues of WT, *lam1* mutant, *WOX9* overexpressing *lam1*, and *WOX9* antisense *lam1* plants (Fig. 3a–d). Transverse sections through the leaf blades showed that the *lam1* leaves had vestigial blade strips at the position of WT blades (Fig. 3f), but these strips were completely absent and blades became fully radialized in *NsWOX9* overexpressing *lam1* lines (Fig. 3g). In *NsWOX9-antisense lam1* lines, however, distinct blade outgrowth was apparent but the nascent blades were not fully expanded compared to the WT leaves (Fig. 3e,h), confirming that blade development in the *NsWOX9-antisense* plants initiated more effectively than in the *lam1* plants but was not completed. Taken together, these results indicate that *WOX9* functions oppose those of *STF/LAM1* in two unrelated eudicot species *M. truncatula* and *N. sylvestris*.

WOX9 overexpression severely affects leaf architecture

To further examine the effect of *WOX9* in leaf blade outgrowth, we introduced *35S::MtWOX9-1*, *35S::MtWOX9-2* and *35S::NsWOX9* into WT *N. sylvestris*. Analysis of over 20 independent transgenic lines for each construct revealed that all transgenic lines displayed an array of leaf phenotypes that can generally be grouped into severe and mild based on the phenotype strength. The WT *N. sylvestris* leaf blade is a well-expanded flat lamina with smooth margin and distinctive pinnate venation pattern (Fig. 4a). *WOX9* overexpression disrupted this pattern resulting in highly disorganized and distorted leaf forms. These include narrow and downward curling blades, deep margin serrations,

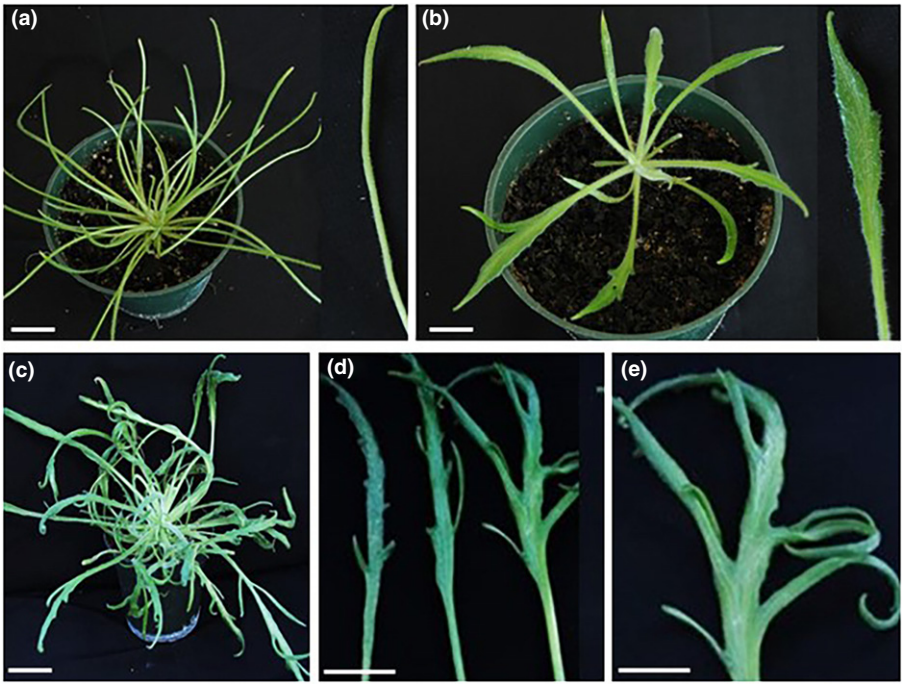

Fig. 2 *NsWOX9-antisense* partially rescues the *lam1* mutant phenotype of *Nicotiana sylvestris*. (a) Phenotype of *lam1* mutant transformed with *35S::GUS* as control at 3 wk of age. Inset on the right is a detached leaf close up. (b) Partially complemented *lam1* phenotype transformed with *35S::NsWOX9-antisense* construct at 3 wk, the inset is a close up of a partially complemented leaf blade. Inset on the right is a detached leaf close up. (c) Partially complemented *lam1* phenotype transformed with *35S::NsWOX9-antisense* construct at 7 wk. (d) Representative individual leaves from *35S::NsWOX9-antisense/lam1* plants. (e) A magnified view of a leaf in (d). Note the branching and curling of leaves especially in older *35S::NsWOX9-antisense/lam1* plants. Bars: (a–d) 5 cm; (e), 1.5 cm.

disorganized venation patterns, uneven blade surfaces, as well as retarded plant growth with two to five tillers and additional leaves leading to a bushy appearance until stem elongation at a later developmental stage (Figs 4b,d,e,g, S4). While most overexpressing plants showed this strong phenotype, some exhibited a mild phenotype where the blade margin, shape and venation patterns were largely intact but with puckered and uneven blade surfaces (Figs 4c,f, S4). *MtWOX9-1* overexpression in *M. truncatula* also produced downward curling and narrower leaves similar to that seen in *N. sylvestris* (Fig. S5), albeit more mild, with an insignificant effect on tillering. Microscopic examination of the leaf epidermal cells revealed that *NsWOX9* overexpressing cells were larger in size, expanded especially in the width direction and the number of cells per unit area was 2–3 times fewer than WT cells (Fig. S6), suggesting that WOX9 may be involved in cell differentiation/expansion. These *WOX9* overexpression phenotypes together suggest that *WOX9* antagonizes the function of *STF/LAM1* in leaf blade outgrowth probably by regulating cell differentiation unlike STF's primary role in cell proliferation (Tadege *et al.*, 2011).

Deleting *NsWOX9* using multiplex gRNA CRISPR/Cas9 genome editing in *N. sylvestris* alters blade symmetry and expansion

To gain insight into the function of the endogenous *WOX9* gene in WT plants, we disrupted *NsWOX9* in *N. sylvestris* using CRISPR/Cas9 genome editing technology. We constructed an *NsWOX9*-multiplex gRNA-CRISPR/Cas9 vector containing three guide RNAs; gRNA1, gRNA2 and gRNA3 (Fig. 5a), and introduced this construct into *N. sylvestris*. Sixteen putative mutant lines were identified by PCR amplification of the target regions using specific primers and Sanger sequencing. Out of these 16 putative mutants, five representative lines were selected for further characterization of their mutant phenotypes (Fig. 5b). Target site sequence analysis of the five *NsWOX9*-CRISPR-mutants labeled here as *NsWOX9-1*, *NsWOX9-2*, *NsWOX9-13*, *NsWOX9-18 and NsWOX9-22* using SeqMan Pro 15.0.1 (DNASTAR software) revealed four different patterns of deletions ranging from 14 to 183 bp (Fig. 5b). *NsWOX9-1* and *NsWOX9-13* had identical 14 bp deletions in gRNA3 and considered as one line. *NsWOX9-2* showed two deletion events at gRNA2 and gRNA3 with 7 and 21 bp deletions, respectively. *NsWOX9-22* showed a 73 bp deletion spanning the upstream and downstream region of gRNA3, while the largest deletion was detected in line *NsWOX9-18* where a 183 bp region between gRNA1 and gRNA2 was removed, which included the PAM region of gRNA1 and extended to three nucleotides upstream of the PAM of gRNA2 (Fig. 5b). All of these CRISPR-derived mutant lines displayed malformed leaves including narrow blades, blade asymmetry, partial deletion in the blade half, rough blade surface, leaf shape distortions, multiple tillers, early flowering and sterility (Fig. 5c–i), indicating that *NsWOX9* is required for bilateral symmetry and proper leaf blade development in *N. sylvestris*.

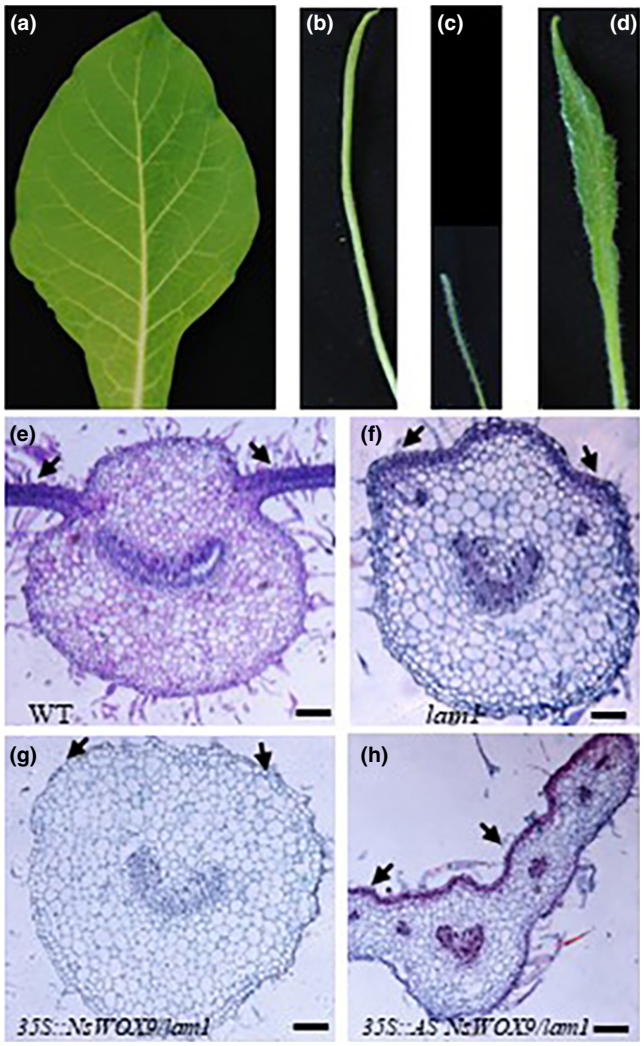

Fig. 3 Transverse section of the leaf blade showing enhancement of the *lam1* blade by *35S::NsWOX9* and partial complementation by *35S::NsWOX9-antisense*. (a) *Nicotiana sylvestris* wild-type (WT) leaf blade. (b) Leaf blade of untransformed *lam1* mutant control. (c) Leaf blade of *lam1* transformed with *35S::NsWOX9*. (d) Partially complemented leaf blade of *lam1* transformed with *35S::NsWOX9-antisense*. (e) Transverse section of *N. sylvestris* WT leaf blade. (f) Transverse section of untransformed *lam1* mutant leaf blade. (g) Transverse sections of *lam1* leaf blade transformed with *35S::NsWOX9* showing radialized blade. (h) Transverse sections of *lam1* leaf blade transformed with *35S::NsWOX9-antisense* showing blade outgrowth. Arrows indicate blade tissue in (e) and (h), vestigial blade stripes in (f) and position of blade in (g). Bars, 50 μm.

The *MtWOX9-1* transcript is detected at the leaflet initiation site and abaxially expressed in leaf primordia but not detected in the SAM

RT-qPCR analysis showed that expression of *MtWOX9-1* was relatively weak in most plant tissues, including leaves, while higher levels of expression were detected in the shoot apex, flowers, pods and immature seeds, with highest levels detected in developing seeds 10 d after anthesis, followed by expression in flowers (Fig. 6a). Highest expression of *MtWOX9-2*, however, was detected in the leaves followed by expression in shoot apices (Fig. S7). However, *MtWOX9-2* is distantly related to *MtWOX9-1* (Fig. S2) and it is not clear at this stage if it performs a redundant function other than the overexpression phenotypes (Figs 1, 4). To further examine expression in different tissues with a different method, we fused a 3 kb promoter region of *MtWOX9-1* upstream of the translational start codon to the β-glucuronidase (*GUS*) coding region, and transformed it into *Medicago* R108 leaf explants. GUS staining analysis revealed that expression in the mature leaf was relatively weak with particularly strong expression in the pulvinus at the base of the leaflets (Fig. S8a). Expression was detected in the flowers and stems (Fig. S8b,c) but, not in the anthers (Fig. 8c). Intense staining was detected in immature pods and seeds at early stages of development (Fig. S8d,e). Expression in the seed became progressively restricted as the seed develops, and confined only to the hilum in the mature seed (Fig. S8f).

To examine the expression pattern of *MtWOX9-1* in more detail at early stages of leaf development, we performed RNA *in situ* hybridization in the shoot apiece of 3-wk-old *M. truncatula* seedlings using *MtWOX9-1* specific antisense probe. We found that *MtWOX9-1* transcript was detected in leaf primordia and at the boundary region between the SAM and leaf primordia, but absent from the central SAM and axillary meristem (Figs 6b–d, S9). A serial section through the SAM and primordia revealed that the transcript was first detected in the peripheral region of the SAM that marks the position of the emerging primordium (P0) and continued to be expressed in leaf primordia to P5 (Figs 6b,c, S9). At P2 and early P3 stages, expression was detected at the leaflet (LL) initiation site, between leaf primordia and stipule (Fig. S9b), and at the boundary region between the terminal leaflet (TL) and emerging LLs (Fig. S9c). In late P3 and P4, the signal was detected at the basal region of the TL and LLs but not in the petiole (Pet) Fig. S9d,e). Interestingly, in expanded and unexpanded young leaves (late P3 to late P5), expression was found restricted to the abaxial side of the leaf with no signal whatsoever on the adaxial side (Fig. 6e,f). No signal was detected in SAM or leaf primordia in the negative control using sense probe (Fig. 6g). These results indicate that *MtWOX9-1* is an abaxial factor expressed starting very early in initiating leaf primordia but conspicuously absent from the central SAM, suggesting that it may be involved in cell differentiation during leaf morphogenesis and development.

MtWOX9-1 is directly repressed by STF in *M. truncatula*

To investigate the mechanistic relationship between *WOX9* and key regulators of blade outgrowth, we examined the leaf blade expression levels of *WOX9* in *stf-2*, *lam1*, and *wox1 prs*, mutants of *M. truncatula*, *N. sylvestris*, and *Arabidopsis thaliana* respectively. RT-qPCR analyses showed that expression of *MtWOX9-1*, *NsWOX9*, and *AtWOX9* was upregulated by 2–4 fold in the leaves of *stf-2*, *lam1* and *wox1 prs* mutants compared to their respective WT levels (Fig. 6h–j), indicating that *WOX9* may be directly or indirectly repressed by the action of STF/LAM1/WOX1 in WT leaves.

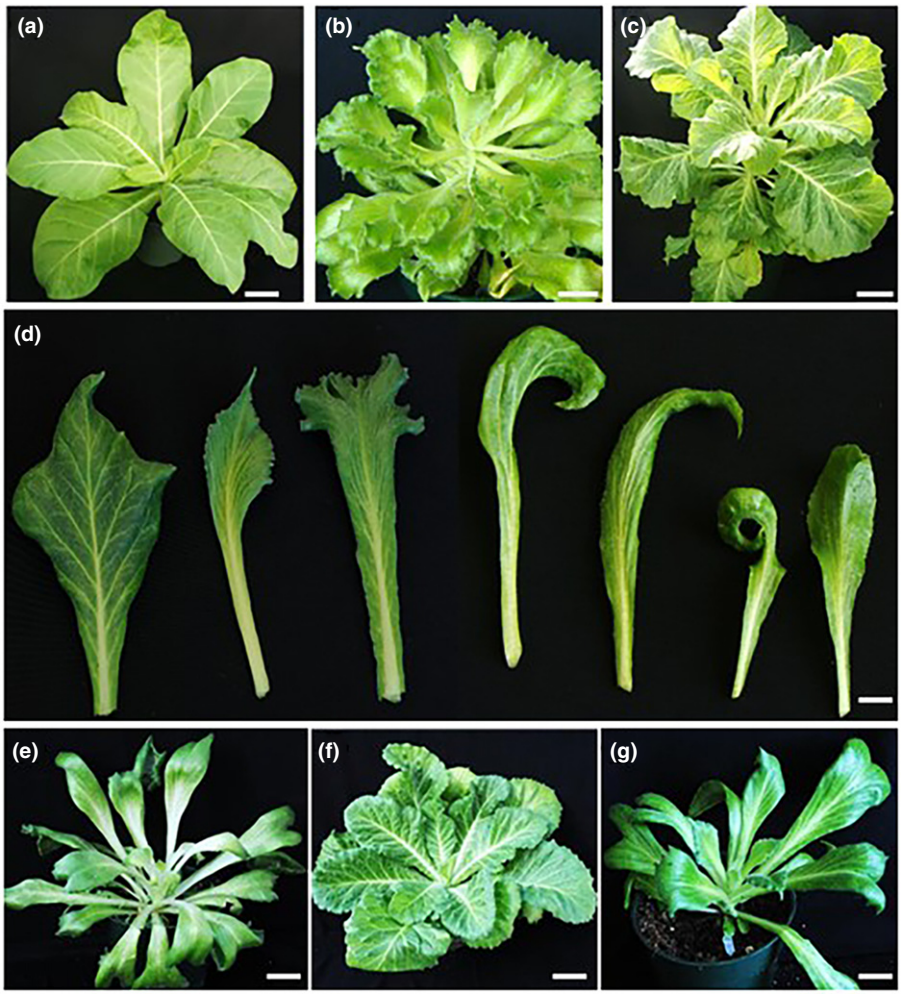

Fig. 4 *WOX9* ectopic expression in wild-type (WT) *Nicotiana sylvestris* alters leaf architecture. (a) WT *N. sylvestris* control plant at 7 wk. (b) Phenotype of *35S::MtWOX9-1*/WT (severe phenotype) at 7 wk after regeneration. (c) Phenotype of *35S::MtWOX9-1*/WT (mild-phenotype) at 7 wk after regeneration. (d) Phenotypes of different individual representative leaves from different *35S::MtWOX9-1*/WT plants showing severe phenotypes at variable stages. (e) Phenotype of *35S::MtWOX9-2*/WT (severe phenotype) at early growth stage. (f) Phenotype of *35S::MtWOX9-2*/WT (mild) at early growth stage. (g) Phenotype of *35S::NsWOX9*/WT (severe) at early growth stage. Bars: (a–c) , (e–g) 10 cm; (d) 3 cm.

To examine whether *MtWOX9-1* is a direct target of STF, we performed a dexamethazone (DEX) induction experiment using the glucocorticoid (GR) system in the presence of the protein synthesis inhibitor, cycloheximide (CHX). Analysis was performed in 4-wk-old *stf* mutant plants transformed with the *35S::YFP-GR-STF* construct. The shoot apex and young leaves of the transgenic plants were treated with both DEX and CHX for 3 h, and *MtWOX9-1* transcript accumulation was monitored by RT-qPCR in the leaves with and without the induction treatment. Our results showed that the expression of *MtWOX9-1* was reduced by *c.* 60% in the DEX and CHX treated lines compared to the control CHX alone (Fig. 7a). Since new protein synthesis is inhibited by CHX in the treated lines, this result suggests that *MtWOX9-1* may be directly repressed by STF. We repeated this experiment in *N. sylvestris* using *35S::YFP-GR-LAM1 c.* 60% repression of *NsWOX9* upon *LAM1* induction by DEX plus CHX treatment (Fig. 7b). However, in the reciprocal experiment, induction of *NsWOX9* expression had no significant effect on *LAM1* expression (Fig. 7c), indicating that *NsWOX9* does not regulate *LAM1* transcription. While *NsWOX9* induction gave a typical *WOX9* overexpression phenotype in the sprayed leaf after 1 wk (Fig. S10a,b), *LAM1* induced leaves looked normal (Fig. S10c,d). We also looked at the transcript level of *LAM1* and *NsWOX9* by semi-quantitative RT-PCR using UBI as a loading control in two *NsWOX9* stable overexpression lines, two *NsWOX9* CRISPR lines and *lam1* mutant. Consistent with the GR induction results, we found that *LAM1* expression was not affected in the *NsWOX9* overexpression and knockout lines (Fig. S11).

To determine if STF reduces *MtWOX9-1* transcript accumulation by targeting its promoter, we performed dual luciferase assay in Arabidopsis protoplasts using the Firefly-Renilla Dual-Luciferase assay system (Promega). In the reporter construct, a 1 kb promoter region of *MtWOX9-1* upstream of the translation start codon was fused to a mini 35S promoter driving the luciferase reporter gene (Fig. 7d), while the effector constructs were made using either STF, or GUS as control, both driven by the 35S promoter (Fig. 7d). Consistent with the earlier results, co-expression of the STF effector in the protoplast almost fully abolished luciferase luminescence compared to the GUS effector control (Fig. 7e), indicating that this 1 kb region of the *MtWOX9-1* promoter is sufficient for STF-dependent repression of transcription.

To determine if STF indeed binds to the *MtWOX9-1* promoter *in vitro* and *in vivo*, we performed EMSA using biotin labeled probes, and ChIP assay, using anti GFP antibody. We previously reported that STF binds preferentially to 'AT-rich' DNA elements

(a)

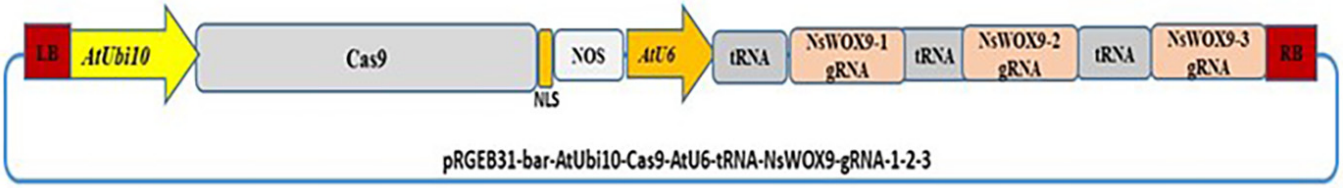

(b)

Mutant name	Mutation events at target site of five homozygous lines			No of nucleotides deleted		
	gRNA1	gRNA2	gRNA3	gRNA1	gRNA2	gRNA3
WT Sequence	CTTCAAGAATATGGCCAAGTTGG	AAATCCTCCCCGAATTCTACTGG	TCTCCTGCTGTTATCACACAAGG	-	-	-
NsWOX9-1	CTTCAAGAATATGGCCAAGTTGG	AAATCCTCCCCGAATTCTACTGG	TCTCCT_____GG	-	-	-14d
NsWOX9-2	CTTCAAGAATATGGCCAAGTTGG	AAATCCTCCCCGAATTC_____	_____AGG	-	-7d	-21d
NsWOX9-13	CTTCAAGAATATGGCCAAGTTGG	AAATCCTCCCCGAATTCTACTGG	TCTCCT_____GG	-	-	-14d
NsWOX9-18	CTTCAAGAATATGGCCA_____/183/_____TACTGG		TCTCCTGCTGTTATCACACAAGG	-183d		-
NsWOX9-22	CTTCAAGAATATGGCCAAGTTGG	AAATCCTCCCCGAATTCTACTGG	_____/73/_____	-	-	-73d

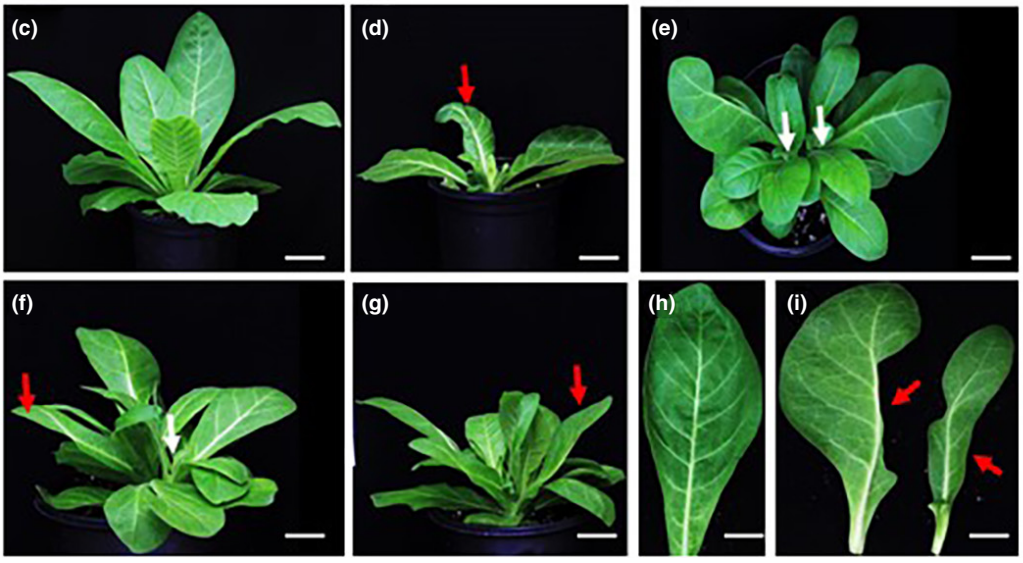

Fig. 5 Knock out of *NsWOX9* with multiplex *gRNA-CRISPR/Cas9* in *Nicotiana sylvestris* alters leaf architecture and symmetry. (a) Schematic representation of the three guide RNAs *NsWOX9*-gRNA1, -gRNA2 and -gRNA3 inserted in pRGEB31-bar-AtUbi10-AtU6-tRNA-gRNA vector. (b) Mutation events detected at the corresponding target sites of gRNA1, gRNA2 and gRNA3 in five independent CRISPR/Cas lines (*NsWOX9-1*, *NsWOX9-2*, *NsWOX9-13*, *NsWOX9-18* and *NsWOX9-22*). (c–i) Phenotype of CRISPR/Cas9 edited plants and leaves; wild-type (WT) control (c), edited *NsWOX9-13* mutant (d), edited *NsWOX9-22* mutant (e), edited *NsWOX9-18* mutant (f), edited *NsWOX9-2* mutant (g), control WT leaf blade (h), representative individual leaf blades from edited plants (i); left, half blade deleted (*NsWOX9-22*), and right, narrow and asymmetric blade (*NsWOX9-2*). Red arrows point to blade defects, white arrows show multiple shoots. Bars: (c–g) 5 cm; (h), (i) 2.5 cm.

without a strong consensus sequence (Zhang *et al.*, 2014). We screened six such selected regions in the 3 kb upstream region of the *MtWOX9-1* promoter, and found that the MBP-STF fusion protein was able to bind to three of them (Fig. 8a). These STF-binding elements are located at −22, −226 and −491 bp upstream of the *MtWOX9-1* CDS while binding was not detected with the control MBP alone (Fig. 8b). Each of these sites were significantly competed by addition of 50-fold excess of the respective unlabeled probes, indicating binding specificity. This shows that, at least *in vitro*, STF can directly bind to multiple sites within the 1 kb fragment of the *MtWOX9-1* promoter, consistent with the dual luciferase assay and GR induction experiments.

To confirm that STF binds to the *MtWOX9-1* promoter *in vivo*, we performed ChIP assays in leaves of Arabidopsis *wox1 prs* double mutant plants transformed with *pMtWOX9-1::MtWOX9-1* construct. Protoplasts were isolated from these transgenic plants and transformed with *35S::STF-GFP* fusion from which chromatin was isolated for analysis. ChIP-qPCR analysis revealed that among the three tested promoter regions (P1, P2 and P3), STF was highly enriched at P2 with significant enrichment also at P3 (Fig. 8c). By contrast, no significant enrichment was detected at P1 or within the *MtWOX9-1* coding region (C1), indicating that STF binds strongly at the P2 position and to a limited extent at the P3 region *in planta*. Taken together, these results indicate that STF directly binds to the proximal region of the *MtWOX9-1* promoter in *M. truncatula*, and represses its activity, and that STF and WOX9 function antagonistically to regulate leaf blade outgrowth.

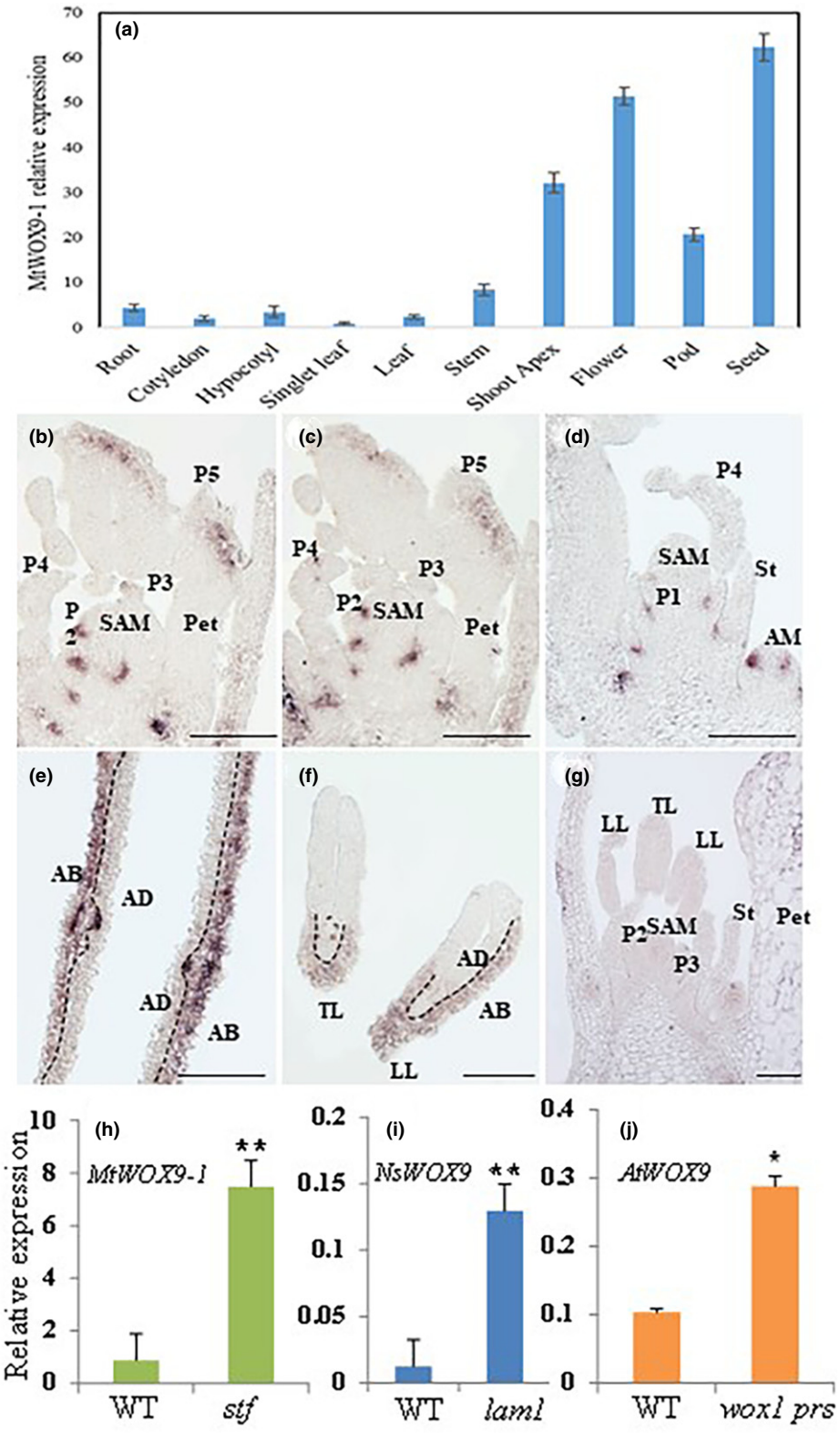

Fig. 6 *MtWOX9-1* is abaxially expressed in leaf primordia and strongly upregulated in the *stf* mutant leaf of *Medicago truncatula* and corresponding mutants in *Nicotiana sylvestris* and Arabidopsis. (a) RT-qPCR analysis showing relative expression of *MtWOX9-1* in different tissues of *M. truncatula*. Leaf, stem, and shoot apex were from 4-wk-old plants, pods and seeds were 10 d after pollination, flower at anthesis, all the rest were at seedling stage. (b–f) RNA *in situ* hybridization in vegetative shoot apex of 3-wk-old *M. truncatula* seedlings using *MtWOX9-1* antisense probe. (b, c) Continuous slice of the SAM in a longitudinal view. (d) Longitudinal section of the SAM viewed from a different angle to show the AM. (e) Expanded young leaf. (f) Unexpended immature leaf. (g) Control with *MtWOX9-1* sense probe. Bars, 50 μm. P1–P5: different developmental stages of the leaf primordia. Pet, petiole; SAM, shoot apical meristem; AM, axillary meristem; St, stipule; TL, terminal leaflet; LL, lateral leaflet; AD,adaxial; AB, abaxial. (h) Relative expression of *MtWOX9-1* in the leaf of 4-wk-old *M. truncatula stf-2* mutant. (i) Relative expression of *NsWOX9* in the leaf of 4-wk-old *Nicotiana sylvestris lam1* mutant. (j) Relative expression of *AtWOX9* in the leaf of 4-wk-old Arabidopsis *wox1 prs* double mutant. Error bars indicate ± SE ($n = 3$). Asterisks indicate significant difference from the control (*, $P < 0.05$; **, $P < 0.01$; Student's *t*-test).

Discussion

Plant specific WOX transcription factors regulate a variety of plant developmental programs from embryogenesis to shoot apical meristem maintenance and lateral organ development (Mayer *et al.*, 1998; Schoof *et al.*, 2000; Lohmann *et al.*, 2001; Matsumoto & Okada, 2001; Nardmann *et al.*, 2004; Sarkar *et al.*, 2007; Breuninger *et al.*, 2008; Shimizu *et al.*, 2009;

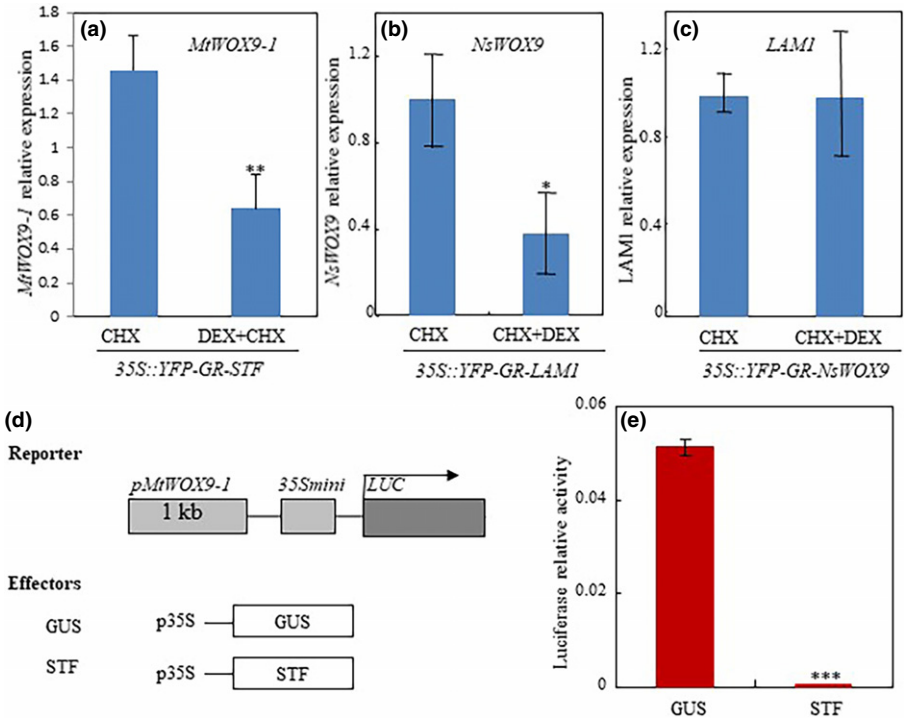

Fig. 7 *WOX9* expression is directly repressed by GR induction of STF or LAM1 in the presence of cyclohexamide, and by STF in Dual Luciferase assay. (a) Relative expression of *MtWOX9-1* in *35S::YFP-GR-STF* transformed *Medicago truncatula* lines with CHX or DEX + CHX treatment for 3 h in 4-wk-old leaves. (b) Relative expression of *NsWOX9* in two independently transformed *35S::YFP-GR-LAM1 Nicotiana sylvestris* lines with CHX alone, CHX + DEX or DEX alone treatments for 6 h in 4-wk-old leaves. (c) Relative expression of *LAM1* in *35S-YFP-GR-NsWOX9* transformed two independent *N. sylvestris* lines with CHX alone, CHX + DEX or DEX alone treatments for 6 h in 4-wk-old young leaves. Relative gene expression was determined by RT-qPCR analyses. (d) Schematic representation of reporter and effector constructs used in the dual luciferase assay. (e) Relative expression of luciferase activity (luminescence) in the presence of 35S::STF effector compared with the 35S::GUS control in Arabidopsis protoplasts. Error bars indicate ± SE ($n = 3$). Asterisks indicate significant difference from the control (*, $P < 0.05$; **, $P < 0.01$; ***, $P < 0.001$; Student's *t*-test).

Vandenbussche *et al.*, 2009; Ji *et al.*, 2010; Tadege *et al.*, 2011a; Nakata *et al.*, 2012). WOX family members are also known for their promiscuous ability to substitute for each other's functions. For example, in Arabidopsis, WUS complements the *prs/wox3* and *wox5* mutants, which are defective in floral organ development and root apical meristem maintenance, respectively (Sarkar *et al.*, 2007; Shimizu *et al.*, 2009). Conversely, members of the WUS clade WOX genes (*WOX1–WOX7*), with the exception of *WOX4*, can substitute for *WUS* function in stem cell maintenance (Dolzblasz *et al.*, 2016). Arabidopsis *WUS* and *WOX1–WOX7* can also complement the *lam1* leaf blade mutant of *N. sylvestris* (Tadege *et al.*, 2011a; Lin *et al.*, 2013a). Here we show that the *M. truncatula* and *N. sylvestris WOX9* homologs, *MtWOX9-1*, *MtWOX9-2* and *NsWOX9* function antagonistically to *STF/LAM1* in regulating leaf blade outgrowth. Ectopic expression of these genes enhanced the *stf* and *lam1* leaf mutant phenotypes, and severely affected blade expansion and morphology in WT *N. sylvestris* with a range of phenotypes (Figs 1, 4). Conversely, reducing *NsWOX9* transcript levels in the *lam1* mutant with antisense technology partially complemented the mutant phenotype (Fig. 2), indicating that *WOX9* antagonizes the *STF/LAM1* function. Complete knockout of *NsWOX9* by CRISPR/Cas9 genome editing in the WT background resulted in a range of leaf blade deformations including lack of bilateral symmetry, altered venation patterns, narrow blades and bushy shoots (Fig. 5), indicating that WOX9 function is required for proper leaf blade development.

In petunia and tomato, *WOX9* homologs are involved in inflorescence development and architecture (Lippman *et al.*, 2008; Rebocho *et al.*, 2008; Costanzo *et al.*, 2014). Both the *evergreen* (*evg*) mutant in petunia (Rebocho *et al.*, 2008) and *compound inflorescence* (*s*) in tomato (Lippman *et al.*, 2008), which dramatically alter the WT inflorescence architecture are caused by lesions in *WOX9* homologs. The *s* allele in tomato results in a highly branched structure with hundreds of flowers, which increases fruit production and may have been selected by breeders (Lippman *et al.*, 2008). In the *evg* mutant of petunia, however, the inflorescence stem often fails to bifurcate after the formation of bracts and continues to grow as a single thickened stem without physical separation of the FM and inflorescence meristem (IM), leading to a fasciated appearance (Rebocho *et al.*, 2008). Unlike *s*, the *evg* FM also fails to produce floral organs suggesting that EVG is required for inflorescence bifurcation and floral organ identity, though *evg* mutants are indistinguishable from WT during early vegetative growth (Rebocho *et al.*, 2008). Thus, in tomato and petunia, *WOX9* homologs appear to have opposite effects specific to inflorescence development and architecture. However, both tomato and petunia have a cymose inflorescence pattern (determinate growth) and it is unclear whether these inflorescence-associated defects are specific to cymose or are also

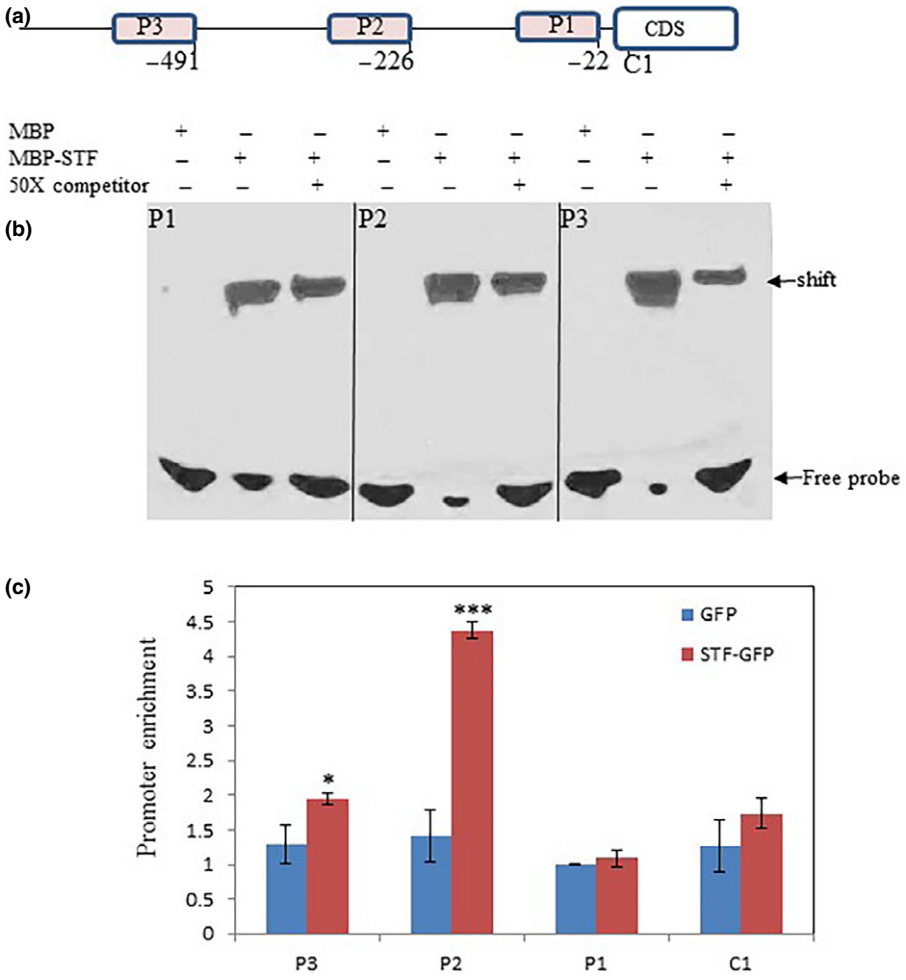

Fig. 8 STF directly binds to the *MtWOX9-1* promoter in EMSA and ChIP assays. (a) Schematic representation of the *MtWOX9-1* promoter and CDS regions tested for EMSA and ChIP assays. The three promoter regions tested are indicated as P1, P2 and P3 and the *MtWOX9-1* coding region as C1. (b) EMSA showing MBP-STF bound to the biotin-labeled probe at P1, P2 and P3 promoter fragments but not the MBP control alone. Fifty-fold excess of unlabeled P1, P2 or P3 DNA was used to compete with the respective labeled probe (right lanes). (c) *MtWOX9-1* promoter enrichment at P1, P2, P3 regions and CDS C1. Chromatin precipitated with anti-GFP antibody from *35S::STF-GFP* and *35S::GFP* control Arabidopsis lines were compared. Purified DNA from the chromatin were used as templates for qPCR. Note that P2 is highly enriched in *35S::STF-GFP* samples. Error bars indicate ± SE ($n = 3$). Asterisks indicate statistical significance (*, $P < 0.05$; ***, $P < 0.001$; Student's *t*-test).

exhibited by racemose (indeterminate growth) and panicle (mixed inflorescence) inflorescences. At least in Arabidopsis (racemose inflorescence), the role of *WOX9* appears not to be restricted to inflorescence development, and in rice (mixed inflorescence), *WOX9* is involved in uniform tiller growth and development (Wang *et al.*, 2014; Fang *et al.*, 2020).

In Arabidopsis, *WOX9*, also called *STIMPY* (*STIP*), is required for meristem growth and maintenance and positively regulates *WUS* (Wu *et al.*, 2005). Futhermore, *stip* mutants display arrested growth at an early stage of development but can be fully rescued by sucrose (Wu *et al.*, 2005). *STIP/WOX9* is shown to mediate cytokinin signaling during shoot meristem establishment and, together with *WOX2* and *WOX8*, regulates zygote and embryo polarity patterning (Wu *et al.*, 2007; Breuninger *et al.*, 2008; Skylar *et al.*, 2010; Ueda *et al.*, 2011). *WOX9* homologs in other species are also reported to be involved in promoting somatic embryogenesis (Gambino *et al.*, 2011; Tvorogova *et al.*, 2019). The Arabidopsis gain-of-function mutant *stip*-D displays wavy leaf margins and increased number of axillary shoots leading to a bushy phenotype (Wu *et al.*, 2005). This phenotype is similar to the wavy margins and bushy shoots seen in all *MtWOX9-1*, *MtWOX9-2* and *NsWOX9* overexpressing *N. sylvestris* transgenic lines (Fig. 4). We uncovered that *MtWOX9-1* is an abaxial factor expressed on the abaxial side of leaf primordia excluded from the central SAM and axillary meristem (Figs 6, S9). At early stages of development, expression was detected at the boundary region between SAM and leaf primordia, leaf primordia and stipules, and between terminal and lateral leaflet. In older leaf primordia (late P3 and afterwards), expression was detected in the basal region of the terminal and lateral leaflets, notwithstanding abaxial-specific expression. In addition, overexpression of *NsWOX9* in *N. sylvestris* resulted in fewer but laterally enlarged cells compared to WT (Fig. S6), suggesting that WOX9 may be involved in organ separation and cell differentiation in the abaxial side of leaf primordia. This is consistent with the observed effect of WOX9 in leaf development and its antagonistic activity to STF. *STF* is expressed at the adaxial–abaxial junction and promotes cell proliferation (Tadege *et al.*, 2011a). Thus, one aspect of the STF and WOX9 anatagonistic function is that STF promotes cell proliferation in the middle domain while WOX9 promotes cell differentiation in the abaxial domain. Such antagonistic function has been demonstrated between STF and the adaxial factor *AS2* (Zhang *et al.*, 2014). It is conceivable that a similar scenario may exist between STF and the abaxial factor *WOX9* since STF/WOX1 is likely to negatively regulate both adaxial

and abaxial factors to protect the cell proliferation zone in the middle domain from differentiation (Nakata *et al.*, 2012).

The Arabidopsis WOX family has been divided into three clades based on phylogenetic analysis: the modern/WUS clade (*WUS*, *WOX1–7*), intermediate clade (*WOX8*, *WOX9*, *WOX11*, *WOX12*), and ancient clade (*WOX10*, *WOX13*, *WOX14*) (van der Graaff *et al.*, 2009). This classification is largely consistent in other species as well (Zhang *et al.*, 2010; Hao *et al.*, 2019; Wu *et al.*, 2020). The WUS clade members are characterized by an intact WUS box motif (Haecker *et al.*, 2004; Lin *et al.*, 2013a), which is a transcriptional repression motif (Ikeda *et al.*, 2009; Lin *et al.*, 2013a). Members of this group function primarily as transcriptional repressors, are able to complement the *lam1* mutant phenotype (Lin *et al.*, 2013a), and are capable of substituting for *WUS* function in maintaining vegetative and FMs (Dolzblasz *et al.*, 2016). The *WOX1* homologs *M. truncatula STF* and *N. sylvestris LAM1* belong to this clade and function as master regulators of leaf blade outgrowth through a transcriptional repression mechanism in association with the co-repressor *TOPLESS* (Tadege *et al.*, 2011a; Lin *et al.*, 2013a,b; Zhang *et al.*, 2014, 2019). The intermediate and ancient clade members have partial or no WUS box, and do not have transcriptional repression activity in Dual Luciferase assays. As a result, they are unable to rescue the *lam1* mutant (Lin *et al.*, 2013a) nor substitute for *WUS* function (Dolzblasz *et al.*, 2016). Among the intermediate and ancient clades, *AtWOX9* is unique in that it displays the strongest activation activity, and strongly enhances the *lam1* mutant phenotype (Lin *et al.*, 2013a), indicating that transcriptional activation activity modulated by AtWOX9 is antagonistic to LAM1 function. This is consistent with the observation that activation activity at the *STF* expression domain antagonizes *STF* function in blade outgrowth (Zhang *et al.*, 2014, 2019).

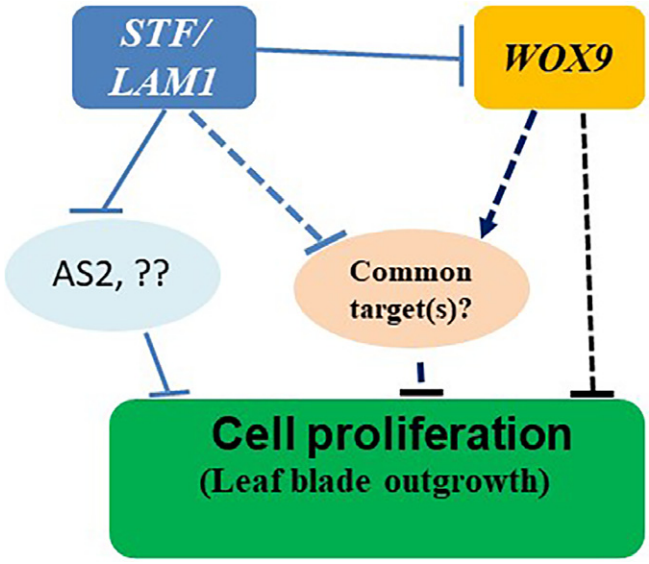

Fig. 9 Schematic representation of hypothetical model for the regulation of cell proliferation-mediated leaf blade outgrowth by the interaction of STF/LAM1 and WOX9. STF/LAM1 directly represses *WOX9, AS2*, and other unidentified cell differentiation factors to promote leaf blade outgrowth through cell proliferation. WOX9, however, antagonizes cell proliferation by activating cell proliferation repressors and/or by promoting cell differentiation. The model proposes that STF/LAM1 and WOX9 may have a common target(s) repressed by STF/LAM1 and activated by WOX9 to achieve homeostasis in cell proliferation and differentiation required for proper blade development during leaf morphogenesis.

The results presented here demonstrated that the *WOX9* transcript is upregulated in three leaf blade mutants; *stf* in *M. truncatula*, *lam1* in *N. sylvestris* and *wox1 prs* in Arabidopsis (Fig. 6j–l), indicating that *WOX9* transcription may be suppressed by STF/LAM1/WOX1 in these species to allow cell proliferation. Several lines of evidence including a GR inducible system in the presence of DEX and CHX, Dual Luciferase assay, EMSA, and ChIP confirmed that STF/LAM1 directly binds to the *MtWOX9-1* promoter to repress *WOX9* transcription (Figs 7, 8), demonstrating that modern clade WOX1/STF/LAM1-mediated repression of intermediate clade *WOX9* is required for proper leaf blade outgrowth in eudicots. In Arabidopsis, *WOX9* functions upstream of *WUS* and is supposed to activate *WUS* to promote vegetative meristem growth (Wu *et al.*, 2005), although it is unclear whether this activation is direct or indirect. *WOX9* is activated by cytokinin signaling (Skylar *et al.*, 2010), and type-B ARRs directly activate *WUS* (Meng *et al.*, 2017; J. Wang *et al.*, 2017; Zhang *et al.*, 2017; Zubo *et al.*, 2017; Xie *et al.*, 2018), while WUS promotes cytokinin activity by repressing type-A ARRs (Leibfried *et al.*, 2005). Thus, cytokinin signaling provides a potential connection between *WOX9* and *WUS* in Arabidopsis, but whether WUS can directly affect *WOX9* activity via negative or positive feedback loop is yet to be determined. Our work clearly demonstrates that in *Medicago* and woodland tobacco, the WUS clade member STF/LAM1 directly represses *MtWOX9-1* or *NsWOX9*, but significant *STF/LAM1* activation by WOX9 was not detected (Fig. 7c). Although MtWOX9-1 may not activate *STF*, it is likely to activate other targets in leaf development. WOX9 amino acid sequences from different species show a highly conserved acidic domain at the C-terminus (Fig. S1), which could mediate transcriptional activation. Thus, our current model is that STF represses the transcription of key targets at the adaxial–abaxial junction to promote cell proliferation, and these targets include cell differentiation factors abaxial *MtWOX9-1* and adaxial *MtAS2* (Zhang *et al.*, 2014). WOX9, however, may positively regulate cell differentiation by directly activating targets independent of STF and/or by activating targets repressed by STF (Fig. 9) but in doing so may negatively regulate cell proliferation. The hypothesis that STF and WOX9 may oppositely regulate common targets providing homeostasis between cell proliferation and differentiation during leaf morphogenesis, explains why WOX9 ectopic expression enhances the *stf lam1* mutant phenotype. Since both STF and WUS promote cell proliferation via a transcriptional repression mechanism in the leaf primordium and SAM, respectively, our findings suggest that direct control of *WOX9* activity by WUS may be required for SAM maintenance as well, uncovering a mechanistic framework for WOX modulated control of robust plant growth and developmental programs. It would be interesting to investigate if repression of the intermediate and ancient clade WOX transcriptional activators by modern clade WOX transcriptional repressors

is a universal strategy exploited during the evolution of land plants and resulting in the complex morphological architecture of flowering plants.

Acknowledgements

This work was supported by the National Science Foundation (NSF) grant IOS-1354422, Agriculture and Food Research Initiative Grant no. 2015-67014-22888 from the USDA National Institute of Food and Agriculture, and the Agricultural Experiment Station. Work in VET's laboratory at St Petersburg State University, Russia, was supported by the Russian Science Foundation project no. 16-16-10011 and by grant from the Russian Foundation for Basic Research no. 20-016-00124.

Author contributions

TWW, HW, and MT designed the research. TWW, HW, DT, FZ, MB, VET, HA, YL, and NC performed the experiments. TWW, HW, FZ, YL, JC, RDA, and MT analyzed the data. TWW, RDA, and MT wrote the manuscript.

ORCID

Randy D. Allen https://orcid.org/0000-0003-2111-2629
Jianghua Chen https://orcid.org/0000-0003-0715-1859
Naichong Chen https://orcid.org/0000-0003-3982-0762
Million Tadege https://orcid.org/0000-0002-3306-3695
Dimiru Tadesse https://orcid.org/0000-0002-5523-3704

References

Asai T, Boller T, Gomez-Gomez L, Sheen J, Ausubel FM, Plotnikova J, Tena G, Chiu WL, Willmann MR. 2002. MAP kinase signalling cascade in Arabidopsis innate immunity. *Nature (London, England). Nature* **415**: 977–983.

Breuninger H, Rikirsch E, Hermann M, Ueda M, Laux T. 2008. Differential expression of WOX genes mediates apical-basal axis formation in the Arabidopsis embryo. *Developmental Cell* **14**: 867–876.

Chen N, Veerappan V, Haggag A, Miyoung K, Allen RD. 2018. HSI2/VAL1 Silences *AGL15* to regulate the developmental transition from seed maturation to vegetative growth in Arabidopsis. *Plant Cell* **30**: 600–619.

Cho S-H, Yoo S-C, Zhang H, Pandeya D, Koh H-J, Hwang J-Y, Kim G-T, Paek N-C. 2013. The rice *narrow leaf2* and *narrow leaf3* loci encode WUSCHEL-related homeobox 3A (OsWOX3A) and function in leaf, spikelet, tiller and lateral root development. *New Phytologist* **198**: 1071–1084.

Costanzo E, Trehin C, Vandenbussche M. 2014. The role of WOX genes in flower development. *Annals of Botany* **114**: 1545–1553.

Daum G, Medzihradszky A, Suzaki T, Lohmann JU. 2014. A mechanistic framework for noncell autonomous stem cell induction in Arabidopsis. *Proceedings of the National Academy of Sciences, USA* **111**: 14619–14624.

Dolzblasz A, Barry C, Brendan D, Elena C, van der Eric G, Jinhui C, Judith N, Thomas L, Wolfgang W. 2016. Stem cell regulation by Arabidopsis WOX Genes. *Molecular Plant* **9**: 1028–1039.

Engler C, Kandzia R, Marillonnet S. 2008. A one pot, one step, precision cloning method with high throughput capability. *PLoS ONE* **3**: e3647.

Fang F, Ye S, Tang J, Bennett MJ, Liang W. 2020. DWT1/DWL2 act together with OsPIP5K1 to regulate plant uniform growth in rice. *New Phytologist* **225**: 1234–1246.

Gambino G, Minuto M, Boccacci P. 2011. Characterization of expression dynamics of WOX homeodomain transcription factors during somatic embryogenesis in *Vitis vinifera*. *Journal of Experimental Botany* **62**: 1089–1101.

Haecker A, Gross-Hardt R, Geiges B, Sarkar A, Breuninger H, Herrmann M, Laux T. 2004. Expression dynamics of WOX genes mark cell fate decisions during early embryonic patterning in *Arabidopsis thaliana*. *Development* **131**: 657–668.

Hao Q, Shan Z, Yang Y, Zhang L, Zhou X-a. 2019. Genome-wide analysis of the WOX gene family and function exploration of *GmWOX18* in soybean. *Plants* **8**: 215.

Ikeda M, Mitsuda N, Ohme-Takagi M. 2009. Arabidopsis *WUSCHEL* is a bifunctional transcription factor that acts as a repressor in stem cell regulation and as an activator in floral patterning. *Plant Cell* **21**: 3493–3505.

Ishiwata A, Akie N, Hiroshi N, Hiro-Yuki H, Makio K, Masahiko M, Misa O, Misuzu N, Sae S-S, Takahiro Y *et al.* 2013. Two WUSCHEL-related homeobox genes, *narrow leaf2* and *narrow leaf3*, control leaf width in rice. *Plant & Cell Physiology* **54**: 779–792.

Iwakawa H, Ueno Y, Semiarti E, Onouchi H, Kojima S, Tsukaya H, Hasebe M, Soma T, Ikezaki M, Machida C *et al.* 2002. The *ASYMMETRIC LEAVES2* gene of *Arabidopsis thaliana*, required for formation of a symmetric flat leaf lamina, encodes a member of a novel family of proteins characterized by cysteine repeats and a leucine zipper. *Plant & Cell Physiology* **43**: 467–478.

Ji J, Strable J, Shimizu R, Koenig D, Sinha N, Scanlon MJ. 2010. *WOX4* promotes procambial development. *Plant Physiology* **152**: 1346–1356.

Kerstetter RA, Bollman K, Taylor RA, Bomblies K, Poethig RS. 2001. *KANADI* regulates organ polarity in Arabidopsis. *Nature* **411**: 706–709.

Kieffer M, Stern Y, Cook H, Clerici E, Maulbetsch C, Laux T, Davies B. 2006. Analysis of the transcription factor *WUSCHEL* and its functional homologue in Antirrhinum reveals a potential mechanism for their roles in meristem maintenance. *Plant Cell* **18**: 560–573.

Laux T, Mayer KF, Berger J, Jürgens G. 1996. The *WUSCHEL* gene is required for shoot and floral meristem integrity in Arabidopsis. *Development* **122**: 87–96.

Lei Y, Lu L, Liu HY, Li S, Xing F, Chen LL. 2014. CRISPR-P: a web tool for synthetic single-guide RNA design of CRISPR-system in plants. *Molecular Plant* **7**: 1494–1496.

Leibfried A, To JP, Busch W, Stehling S, Kehle A, Demar M, Kieber JJ, Lohmann JU. 2005. *WUSCHEL* controls meristem function by direct regulation of cytokinin-inducible response regulators. *Nature* **438**: 1172–1175.

Lin H, Niu L, McHale NA, Ohme-Takagi M, Mysore KS, Tadege M. 2013a. Evolutionarily conserved repressive activity of WOX proteins mediates leaf blade outgrowth and floral organ development in plants. *Proceedings of the National Academy of Sciences, USA* **110**: 366–371.

Lin H, Niu L, Tadege M. 2013b. STENOFOLIA acts as a repressor in regulating leaf blade outgrowth. *Plant Signaling & Behavior* **8**: e24464.

Lippman ZB, Cohen O, Alvarez JP. 2008. The making of a compound inflorescence in tomato and related nightshades. *PLoS Biology* **6**: 2424–2435.

Lohmann JU, Hong RL, Hobe M, Busch MA, Parcy F, Simon R, Weigel D. 2001. A molecular link between stem cell regulation and floral patterning in Arabidopsis. *Cell* **105**: 793–803.

Matsumoto N, Okada K. 2001. A homeobox gene, *PRESSED FLOWER*, regulates lateral axis-dependent development of Arabidopsis flowers. *Genes & Development* **15**: 3355–3364.

Mayer KF, Schoof H, Haecker A, Lenhard M, Jürgens G, Laux T. 1998. Role of *WUSCHEL* in regulating stem cell fate in the Arabidopsis shoot meristem. *Cell* **95**: 805–815.

McConnell JR, Emery J, Eshed Y, Bao N, Bowman J, Barton MK. 2001. Role of *PHABULOSA* and *PHAVOLUTA* in determining radial patterning in shoots. *Nature* **411**: 709–713.

Meng W, Cheng Z, Sang Y, Zhang M, Rong X, Wang Z, Tang Y, Zhang X. 2017. Type-B *ARABIDOPSIS RESPONSE REGULATOR*s specify the shoot stem cell niche by dual regulation of *WUSCHEL*. *Plant Cell* **29**: 1357–1372.

Meng Y, Liu H, Wang H, Liu Y, Zhu B, Wang Z, Hou Y, Zhang P, Wen J, Yang H *et al.* 2019. *HEADLESS*, a WUSCHEL homolog, uncovers novel aspects of shoot meristem regulation and leaf blade development in *Medicago truncatula*. *Journal of Experimental Botany* **70**: 149–163.

Nakata M, Matsumoto N, Tsugeki R, Rikirsch E, Laux T, Okada K. 2012. Roles of the middle domain-specific *WUSCHEL-RELATED HOMEOBOX* genes in early development of leaves in Arabidopsis. *Plant Cell* **24**: 519–535.

Nakata M, Okada K. 2012. The three-domain model: a new model for the early development of leaves in *Arabidopsis thaliana*. *Plant Signaling & Behavior* **7**: 1423–1427.

Nardmann J, Ji J, Werr W, Scanlon MJ. 2004. The maize duplicate genes *narrow sheath1* and *narrow sheath2* encode a conserved homeobox gene function in a lateral domain of shoot apical meristems. *Development* **131**: 2827–2839.

Niu HLX, Tong C, Wang H, Li S, Lu L, Pan Y, Zhang X, Weng Y, Li Z. 2018. The *WUSCHEL-related homeobox1* gene of cucumber regulates reproductive organ development. *Journal of Experimental Botany* **69**: 5373–5387.

Park SO, Zheng Z, Oppenheimer DG, Hauser BA. 2005. The *PRETTY FEW SEEDS2* gene encodes an Arabidopsis homeodomain protein that regulates ovule development. *Development* **132**: 841–849.

Rebocho AB, Bliek M, Kusters E, Castel R, Procissi A, Roobeek I, Souer E, Koes R. 2008. Role of *EVERGREEN* in the development of the cymose petunia inflorescence. *Developmental Cell* **15**: 437–447.

Sarkar AK, Luijten M, Miyashima S, Lenhard M, Hashimoto T, Nakajima K, Scheres B, Heidstra R, Laux T. 2007. Conserved factors regulate signalling in *Arabidopsis thaliana* shoot and root stem cell organizers. *Nature* **446**: 811–814.

Sawa S, Watanabe K, Goto K, Liu YG, Shibata D, Kanaya E, Morita EH, Okada K. 1999. *FILAMENTOUS FLOWER*, a meristem and organ identity gene of Arabidopsis, encodes a protein with a zinc finger and HMG-related domains. *Genes & Development* **13**: 1079–1088.

Schoof H, Lenhard M, Haecker A, Mayer KF, Jürgens G, Laux T. 2000. The stem cell population of Arabidopsis shoot meristems in maintained by a regulatory loop between the *CLAVATA* and *WUSCHEL* genes. *Cell* **100**: 635–644.

Shimizu R, Ji J, Kelsey E, Ohtsu K, Schnable PS, Scanlon MJ. 2009. Tissue specificity and evolution of meristematic *WOX3* function. *Plant Physiology* **149**: 841–850.

Siegfried KR, Eshed Y, Baum SF, Otsuga D, Drews GN, Bowman JL. 1999. Members of the YABBY gene family specify abaxial cell fate in Arabidopsis. *Development* **126**: 4117–4128.

Skylar A, Hong FX, Chory J, Weigel D, Wu XL. 2010. *STIMPY* mediates cytokinin signaling during shoot meristem establishment in Arabidopsis seedlings. *Development* **137**: 541–549.

Snipes SA, Rodriguez K, DeVries AE, Miyawaki KN, Perales M, Xie M, Reddy GV. 2018. Cytokinin stabilizes WUSCHEL by acting on the protein domains required for nuclear enrichment and transcription. *PLoS Genetics* **14**: 1–23.

Stuurman J, Jaggi F, Kuhlemeier C. 2002. Shoot meristem maintenance is controlled by a GRAS-gene mediated signal from differentiating cells. *Genes & Development* **16**: 2213–2218.

Tadege M. 2016. *WOX3* in the scene: intimacy with hormones. *Journal of Experimental Botany* **67**: 1605–1607.

Tadege M, Chen F, Murray J, Wen J, Ratet P, Udvardi M, Dixon R, Mysore K. 2015. Control of vegetative to reproductive phase transition improves biomass yield and simultaneously reduces lignin content in *Medicago truncatula*. *BioEnergy Research* **8**: 857–867.

Tadege M, Lin H, Bedair M, Berbel A, Wen J, Rojas CM, Niu L, Tang Y, Sumner L, Ratet P *et al.* 2011a. *STENOFOLIA* regulates blade outgrowth and leaf vascular patterning in *Medicago truncatula* and *Nicotiana sylvestris*. *Plant Cell* **23**: 2125–2142.

Tadege M, Lin H, Niu L, Mysore KS. 2011b. Control of dicot leaf blade expansion by a WOX gene, STF. *Plant Signal Behavior* **6**: 1861–1864.

Tadege M, Mysore KS. 2011. *Tnt1* retrotransposon tagging of *STF* in *Medicago truncatula* reveals tight coordination of metabolic, hormonal and developmental signals during leaf morphogenesis. *Mobile Genetic Elements* (2159–2543) **1**: 301–303.

Tvorogova VE, Fedorova YE, Potsenkovskaya EA, Kudriashov AA, Efremova EP, Kvitkovskaya VA, Wolabu TW, Zhang F, Tadege M, Lutova LA. 2019. The WUSCHEL-related homeobox transcription factor *MtWOX9-1* stimulates somatic embryogenesis in *Medicago truncatula*. *Plant Cell, Tissue and Organ Culture* **3**: 517–527.

Ueda M, Zhang ZJ, Laux T. 2011. Transcriptional activation of Arabidopsis axis patterning genes *WOX8/9* links zygote polarity to embryo development. *Developmental Cell* **20**: 264–270.

van der Graaff E, Laux T, Rensing SA. 2009. The WUS homeobox-containing (WOX) protein family. *Genome Biology* **10**: 248.

Vandenbussche M, Horstman A, Zethof J, Koes R, Rijpkema AS, Gerats T. 2009. Differential recruitment of WOX transcription factors for lateral development and organ fusion in Petunia and Arabidopsis. *Plant Cell* **21**: 2269–2283.

Waites R, Selvadurai HRN, Oliver IR, Hudson A. 1998. The *PHANTASTICA* gene encodes a MYB transcription factor involved in growth and dorsoventrality of lateral organs in *Antirrhinum*. *Cell* **93**: 779–789.

Wang H, Niu L, Fu C, Meng Y, Sang D, Yin P, Wu J, Tang Y, Lu T, Wang ZY *et al.* 2017. Overexpression of the WOX gene *STENOFOLIA* improves biomass yield and sugar release in transgenic grasses and display altered cytokinin homeostasis. *PLoS Genetics* **13**: e1006649.

Wang H, Xu Y, Hong L, Zhang X, Wang X, Zhang J, Ding Z, Meng Z, Wang ZY, Long R *et al.* 2019. *HEADLESS* regulates auxin response and compound leaf morphogenesis in *Medicago truncatula*. *Frontiers in Plant Science* **10**: 1024.

Wang J, Caihuan T, Cui Z, Bihai S, Xiuwei C, Tian-Qi Z, Zhong Z, Jia-Wei W, Yuling J. 2017. Cytokinin signaling activates *WUSCHEL* expression during axillary meristem initiation. *Plant Cell* **29**: 1373–1387.

Wang W, Li G, Zhao J, Chu H, Lin W, Zhang D, Wang Z, Wwsec Liang. 2014. *DWARF TILLER1*, a WUSCHEL-related homeobox transcription factor, is required for tiller growth in rice. *PLoS Genetics* **10**: 1–15.

Weigel D, Glazebrook J. 2002. *Arabidopsis: a laboratory manual*. New York, NY, USA: Cold Spring Harbor Laboratory Press.

Wu CC, Li FW, Kramer EM. 2020. Large-scale phylogenomic analysis suggests three ancient superclades of the WUSCHEL-RELATED HOMEOBOX transcription factor family in plants. *PLoS ONE* **14**: e0223521.

Wu X, Chory J, Weigel D. 2007. Combinations of WOX activities regulate tissue proliferation during Arabidopsis embryonic development. *Developmental Biology* **309**: 306–316.

Wu XL, Dabi T, Weigel D. 2005. Requirement of homeobox gene *STIMPY/WOX9* for Arabidopsis meristem growth and maintenance. *Current Biology* **15**: 436–440.

Xie K, Minkenberg B, Yang Y. 2015. Boosting CRISPR/Cas9 multiplex editing capability with the endogenous tRNA-processing system. *Proceedings of the National Academy of Sciences, USA* **112**: 3570–3575.

Xie M, Chen H, Huang L, O'Neil R, Shokhirev M, Ecker J. 2018. A B-ARR-mediated cytokinin transcriptional network directs hormone cross-regulation and shoot development. *Nature Communications* **9**: 1604.

Xiong Y, McCormack M, Li L, Hall Q, Xiang C, Sheen J. 2013. Glucose-TOR signalling reprograms the transcriptome and activates meristems. *Nature* **496**: 181–186.

Yadav RK, Perales M, Gruel J, Girke T, Jonsson H, Reddy GV. 2011. WUSCHEL protein movement mediates stem cell homeostasis in the Arabidopsis shoot apex. *Genes & Development* **25**: 2025–2030.

Zhang F, May A, Irish VF. 2017. Type-B Arabidopsis response regulators directly activate *WUSCHEL*. *Trends in Plant Science* **22**: 815–817.

Zhang F, Tadege M. 2015. Repression of *AS2* by WOX family transcription factors is required for leaf development in Medicago and Arabidopsis. *Plant Signal Behavior* **10**: e993291.

Zhang F, Wang H, Kalve S, Wolabu TW, Nakashima J, Golz JF, Tadege M. 2019. Control of leaf blade outgrowth and floral organ development by *LEUNIG*, *ANGUSTIFOLIA3* and *WOX* transcriptional regulators. *New Phytologist* **223**: 2024–2038.

Zhang F, Wang Y, Li G, Tang YK, Tadege EM. 2014. STENOFOLIA recruits TOPLESS to repress *ASYMMETRIC LEAVES2* at the leaf margin and promote leaf blade outgrowth in *Medicago truncatula*. *Plant Cell* **26**: 650–664.

Zhang X, Yin J, Zhang D, Zong J, Liu J. 2010. Genome-wide analysis of WOX gene family in Rice, Sorghum, Maize, Arabidopsis and Poplar [electronic resource]. *Journal of Integrative Plant Biology* **52**: 1016–1026.

Zhuang L-L, Ambrose M, Rameau C, Weng L, Yang J, Hu X-H, Luo D, Li X. 2012. *LATHYROIDES*, encoding a WUSCHEL-related Homeobox1 transcription factor, controls organ lateral growth, and regulates tendril and

dorsal petal identities in garden pea (*Pisum sativum* L.). *Molecular Plant* **5**: 1333–1345.

Zubo YO, Yamburenko MV, Worthen JM, Street IH, Hill K, Schaller GE, Blakley IC, Loraine AE, Franco-Zorrilla JM, Wenjing Z *et al.* 2017. Cytokinin induces genome-wide binding of the type-B response regulator *ARR10* to regulate growth and development in Arabidopsis. *Proceedings of the National Academy of Sciences, USA* **114**: E5995–E6004.

Supporting Information

Additional Supporting Information may be found online in the Supporting Information section at the end of the article.

Fig. S1 Amino acid sequence alignment of MtWOX9-1/2 and other related eudicot WOX9 sequences.

Fig. S2 Phylogenetic analysis of MtWOX9-1/2 and other related eudicots WOX9 protein sequences.

Fig. S3 Ectopic expression of *MtWOX9-1* enhances the *lam1* mutant phenotypes.

Fig. S4 Leaf phenotypes of *NsWOX9* overexpression in *Nicotiana sylvestris*.

Fig. S5 Phenotype of *MtWOX9-1* overexpression in *Medicago truncatula*.

Fig. S6 *NsWOX9* overexpression laterally expands epidermal cell size in *Nicotiana sylvestris*.

Fig. S7 RT-qPCR analysis of *MtWOX9-2* expression in different tissues of *Medicago truncatula*.

Fig. S8 *MtWOX9-1* expression by GUS staining in *MtWOX9-1::GUS* transformed lines of *Medicago truncatula*.

Fig. S9 RNA *in situ* hybridization of *MtWOX9-1* in the vegetative shoot apex and leaf primordia of 3-wk-old *Medicago truncatula* R108 seedlings.

Fig. S10 Leaf phenotypes of *35S::YFP-GR-NsWOX9* and *35S::YFP-GR-LAM1* lines with or without DEX treatment.

Fig. S11 Analysis of *LAM1* and *NsWOX9* expression by semi-quantitative RT-PCR in *NsWOX9* overexpression and knockout lines.

Table S1 List of primers and gRNAs used in this study.

Please note: Wiley Blackwell are not responsible for the content or functionality of any Supporting Information supplied by the authors. Any queries (other than missing material) should be directed to the *New Phytologist* Central Office.